Quantum-like Chaos in Prime Number Distribution and in Turbulent Fluid Flows

A. M. Selvam
(Retired) Indian Institute of Tropical Meteorology
Pune 411 008, India
email: selvam@ip.eth.net
website: http://www.geocities.com/amselvam

Recent studies by mathematicians and physicists have identified a close association between the distribution of prime numbers and quantum mechanical laws governing the subatomic dynamics of quantum systems such as the electron or the photon. It is now recognised that *Cantorian fractal space-time* fluctuations characterise dynamical systems of all space-time scales ranging from the microscopic subatomic dynamics to macro-scale turbulent fluid flows such as atmospheric flows. The spacing intervals of adjacent prime numbers also exhibit *fractal* (irregular) fluctuations generic to dynamical systems in nature. The apparently irregular (chaotic) *fractal* fluctuations of dynamical systems, however, exhibit self-similar geometrical pattern and are associated with inverse power-law form for the power spectrum. Self-similar fluctuations imply long-range space-time correlations identified as *self-organized criticality*. A cell dynamical system model for atmospheric flows developed by the author gives the following important results: (a) *Self-organized*

criticality is a signature of quantum-like chaos (b) The observed *self-organized criticality* is quantified in terms of the universal inverse power-law form of the statistical normal distribution (c) The spectrum of *fractal* fluctuations is a broadband continuum with embedded dominant eddies. The *cell dynamical system model* is a general systems theory applicable to all dynamical systems (real world and computed) and the model concepts are applied to derive the following results for the observed association between prime number distribution and quantum-like chaos. (i) Number theoretical concepts are intrinsically related to the quantitative description of dynamical systems. (ii) Continuous periodogram analyses of different sets of adjacent prime number spacing intervals show that the power spectra follow the model predicted universal inverse power-law form of the statistical normal distribution. The prime number distribution therefore exhibits *self-organized criticality*, which is a signature of quantum-like chaos. (iii) The continuum real number field contains unique structures, namely, *prime numbers*, which are analogous to the dominant eddies in the eddy continuum in turbulent fluid flows.

Keywords: quantum-like chaos in prime numbers, fractal structure of primes, quantification of prime number distribution, prime numbers and fluid flows

1. Introduction

The continuum real number field (infinite number of decimals between any two integers) represented as Cartesian co-ordinates [Mathews, 1961; Stewart and Tall, 1990; Devlin, 1997; Stewart, 1998] is the basic computational tool in the simulation and prediction of the continuum dynamics of real world dynamical systems such as fluid flows, stock market price fluctuations, heart beat patterns, etc. Till the late 1970s, mathematical models were

based on Newtonian continuum dynamics with implicit assumption of linearity in the rate of change with respect to (w. r. t) time or space of the dynamical variable under consideration. The traditional mathematical model equations were of the form

$$X_{n+1} = X_n + \left(\frac{dX}{dt}\right)_n dt \qquad (1)$$

Constant value was assumed for the rate of change $(dX/dt)_n$ of the variable X_n at computational step n and infinitesimally small time or space intervals dt. Equation (1) will be linear and can be solved analytically provided the rate of change $(dX/dt)_n$ is constant. However, dynamical systems in nature exhibit irregular (*fractal*) fluctuations on all space and time scales and therefore the assumption of constant rate of change fails and Equation (1) does not have analytical solution. Numerical solutions are then obtained for discrete (finite) space-time intervals such that the continuum dynamics of Equation (1) is now computed as discrete dynamics given by

$$X_{n+1} = X_n + \left(\frac{\Delta X}{\Delta t}\right)_n \Delta t \qquad (2)$$

Numerical solutions obtained using Equation (2), which is basically a numerical integration procedure, involve iterative computations with feedback and amplification of round-off error of real number finite precision arithmetic. The Equation (2) also represents the relationship between continuum number field and embedded discrete (finite) number fields. Numerical solutions for non-linear dynamical systems represented by Equation (2) are sensitively dependent on initial conditions and give apparently chaotic solutions, identified as *deterministic chaos*. *Deterministic chaos* therefore characterises the evolution of discrete (finite) structures from the underlying continuum number field.

Historically, sensitive dependence on initial conditions of non-linear dynamical systems was identified nearly a century ago by *Poincare* (Poincare, 1892) in his study of three-body problem, namely the sun, earth and the moon. Non-linear dynamics remained a neglected area of research till the advent of electronic computers in the late 1950s. Lorenz, in 1963 showed that numerical solutions of a simple model of atmospheric flows exhibited sensitive dependence on initial conditions implying loss of predictability of the future state of the system. The traditional non-linear dynamical system defined by Equation (2) is commonly used in all branches of science and other areas of human interest. *Non-linear dynamics and chaos* soon (by 1980s) became a multidisciplinary field of intensive research (Gleick, 1987). Sensitive dependence on initial conditions implies long-range space-time correlations. The observed irregular fluctuations of real world dynamical systems also exhibit such non-local connections manifested as *fractal* or *self-similar* geometry to the space-time evolution. The universal symmetry of *self-similarity* ubiquitous to dynamical systems in nature is now identified as *self-organized criticality* (Bak, Tang and Wiesenfeld, 1988). A symmetry of some figure or pattern is a transformation that leaves the figure invariant, in the sense that, taken as a whole it looks the same after the transformation as it did before, although individual points of the figure may be moved by the transformation (Devlin, 1997). *Self-similar* structures have internal geometrical structure, which resemble the whole. The space-time organization of a hierarchy of *self-similar* space-time structures is common to real world as well as the numerical models (Equation 2) used for simulation. A substratum of continuum fluctuations self-organizes to generate the observed unique hierarchical structures both in real world and the continuum number field used as the tool for simulation. A *cell dynamical system model* developed by the author [Mary Selvam, 1990; Selvam and Suvarna

Fadnavis, 1998; 1999a;b] for turbulent fluid flows shows that *self-similar* (*fractal*) space-time fluctuations exhibited by real world and numerical models of dynamical systems are signatures of quantum-like mechanics. The model concepts are independent of the exact details, such as, the chemical, physical, physiological, etc., properties of the dynamical systems and therefore provide a general systems theory (Peacocke, 1989; Klir, 1993; Jean, 1994) applicable for all dynamical systems in nature. The model concepts are applicable to the emergence of unique prime number spectrum from the underlying substratum of continuum real number field.

Recent studies indicate a close association between *number theory* in mathematics, in particular, the distribution of *prime numbers* and the chaotic orbits of excited quantum systems such as the hydrogen atom [Keating, 1990; Cipra, 1996; Klarreich, 2000]. Mathematical studies also indicate that *Cantorian fractal* space-time characterises quantum systems [Ord, 1983; Nottale, 1989; El Naschie, 1993]. The *fractal* fluctuations exhibited by prime number distribution and microscopic quantum systems belong to the newly identified science of *non-linear dynamics and chaos*. Quantification of the apparently irregular (chaotic) *fractal* fluctuations will help compute (predict) the space-time evolution of the fluctuations. The *cell dynamical system model* concepts described below (Section 2) provide a theory for unique quantification of the observed *fractal* fluctuations in terms of the universal inverse power-law form of the statistical normal distribution.

2. Cell Dynamical System Model Concepts

The model concepts are based on Townsend's [Townsend, 1956] visualization of large eddies as envelopes enclosing turbulent eddy (small-scale) fluctuations (Figure 1). The relationship between root

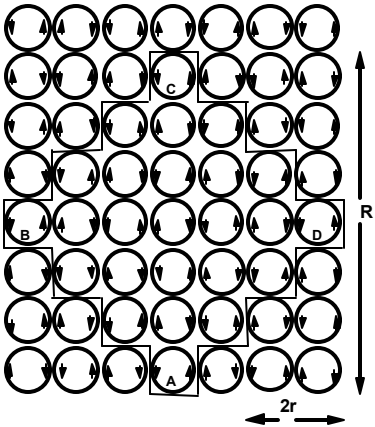

Figure 1: Visualisation of the formation of large eddy (ABCD) as envelope enclosing smaller scale eddies. By analogy, the continuum number field domain (Cartesian co-ordinates) may also be obtained from successive integration of enclosed finite number field domains.

mean square (r.m.s.) circulation speeds W and w_* respectively of large and turbulent eddies of respective radii R and r is then given as

$$W^2 = \frac{2}{\pi}\frac{r}{R}w_*^2 \qquad (3)$$

The dynamical evolution of space-time fractal structures is quantified in terms of ordered energy flow between fluctuations of all scales in Equation (3), because the square of the eddy circulation speed represents the eddy energy (kinetic). A hierarchical continuum of eddies is generated by the integration of successively larger enclosed turbulent eddy circulations and therefore the eddy energy (kinetic) spectrum follows statistical normal distribution according to the *Central Limit Theorem* [Ruhla, 1992; see Section 2.1(e) below]. Therefore, square of the eddy amplitude or the variance represents the probability. Such a result that the additive amplitudes of eddies, when squared, represent the probability densities is observed for the subatomic dynamics of quantum systems such as the electron or photon (Maddox 1988). Townsend's visualisation of large eddy

structure as quantified in Equation (3) leads to the most important result that the self-similar *fractal* fluctuations of atmospheric flows are manifestations of quantum-like chaos.

2.1 Cell Dynamical System Model Predictions

A summary of the important theoretical results derived from Equation (3) [Mary Selvam, 1990; Selvam and Suvarna Fadnavis, 1998; 1999a; b], which are applicable to the present study, is given in the following.

(a) The fractal structure of the continuum flow pattern is resolved into an overall logarithmic spiral trajectory $R_oR_1R_2R_3R_4R_5$ with the quasiperiodic *Penrose* tiling pattern for the internal structure and is equivalent to a hierarchy of vortices (Figure 2). The successively larger eddy radii (OR_o, OR_1, etc.) and the corresponding circulation speeds (W_1, W_2 etc.) follow the *Fibonacci* mathematical series. A brief summary of details of *Penrose* tiling pattern relevant to the present study is given in the following.

Historically, the British mathematician *Roger Penrose* discovered in 1974 the quasiperiodic *Penrose* tiling pattern, purely as a mathematical concept. The fundamental investigation of tilings, which fill space completely, is analogous to investigating the manner in which matter splits up into atoms and natural numbers split up into product of primes. The distinction between periodic and aperiodic tilings is somewhat analogous to the distinction between rational and irrational real numbers, where the latter have decimal expansions that continue forever, without settling into repeating blocks [Devlin, 1997]. Even earlier *Kepler* saw a fundamental mathematical connection between symmetric patterns and 'space filling geometric figures' such as his own discovery, the *rhombic dodecahedron*, a figure having 12 identical faces [Devlin, 1997]. The quasiperiodic *Penrose* tiling

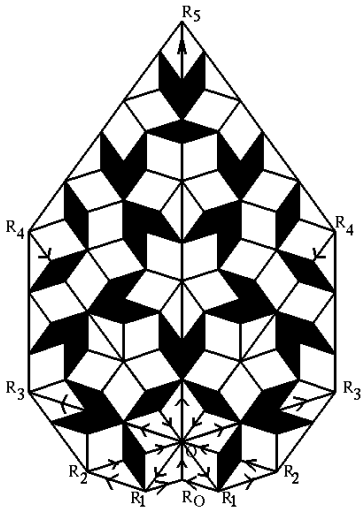

Figure 2: The quasiperiodic Penrose tiling pattern with five-fold symmetry traced by the small eddy circulations internal to dominant large eddy circulation in turbulent fluid flows.

pattern has five-fold symmetry of the dodecahedron. Recent studies [Seife, 1998] show that in a strong magnetic field, electrons swirl around magnetic field lines, creating a vortex. Under right conditions, a vortex can couple to an electron, acting as a single unit. Vortex geometrical structure is ubiquitous in macro-scale as well as microscopic subatomic dynamical fluctuation patterns.

(b) Conventional continuous periodogram power spectral analyses of such spiral trajectories in Figure 2 ($R_oR_1R_2R_3R_4R_5$) will reveal a continuum of periodicities with progressive increase $d\theta$ in phase angle θ (theta) as shown in Figure 3.

(c) The broadband power spectrum will have embedded dominant wavebands (R_oOR_1, R_1OR_2, R_2OR_3, R_3OR_4, R_4OR_5, etc.) the bandwidth increasing with period length (Figure 2). The peak periods E_n in the dominant wavebands is be given by the relation

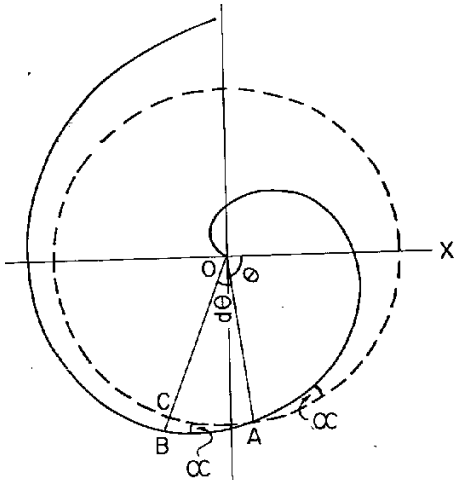

Figure 3: The equiangular logarithmic spiral given by $(R/r) = \exp(\alpha\theta)$ where α and θ are each equal to $1/z$ for each length step growth. The eddy length scale ratio z is equal to R/r. The crossing angle α is equal to the small increment $d\theta$ in the phase angle θ. Traditional power spectrum analysis will resolve such a spiral flow trajectory as a continuum of eddies with progressive increase $d\theta$ in phase angle θ.

$$E_n = T_s(2 + \tau)\tau^n \qquad (4)$$

where τ is the *golden mean* equal to $(1+\sqrt{5})/2$ [approximately equal to 1.618] and T_s , the primary perturbation time period, for example, is the annual cycle (summer to winter) of solar heating in a study of atmospheric interannual variability. The peak periods E_n are superimposed on a continuum background. For example, the most striking feature in climate variability on all time scales is the presence of sharp peaks superimposed on a continuous background [Ghil, 1994].

(d) The ratio r/R also represents the increment $d\theta$ in phase angle θ (Equation 3 and Figure 3) and therefore the phase angle θ represents the variance [Mary Selvam, 1990]. Hence, when the logarithmic spiral is resolved as an eddy continuum in conventional spectral analysis, the increment in wavelength is concomitant with increase in phase. The angular turning, in turn, is directly proportional to the variance (Equation 3). Such a result

that increments in wavelength and phase angle are related is observed in quantum systems and has been named '*Berry's phase*' [Berry, 1988]. The relationship of angular turning of the spiral to intensity of fluctuations is seen in the tight coiling of the hurricane spiral cloud systems.

(e) The overall logarithmic spiral flow structure is given by the relation

$$W = \frac{w_*}{k} \log z \tag{5}$$

where the constant k is the steady state fractional volume dilution of large eddy by inherent turbulent eddy fluctuations. The constant k is equal to $1/\tau^2 (\approx 0.382)$ and is identified as the universal constant for deterministic chaos in fluid flows [Mary Selvam, 1990]. Since k is less than half, the mixing with environmental air does not erase the signature of the dominant large eddy, but helps to retain its identity as a stable self-sustaining *soliton-like* structure. The mixing of environmental air assists in the upward and outward growth of the large eddy. The steady state emergence of fractal structures is therefore equal to

$$1/k \approx 2.62 \tag{6}$$

Logarithmic wind profile relationship such as Equation 5 is a long-established (observational) feature of atmospheric flows in the boundary layer, the constant k, called the *Von Karman* 's constant has the value equal to 0.38 as determined from observations [Wallace and Hobbs, 1977]. In Equation 5, W represents the standard deviation of eddy fluctuations, since W is computed as the instantaneous r.m.s. (root mean square) eddy perturbation amplitude with reference to the earlier step of eddy growth. For two successive stages of eddy growth starting from primary perturbation w_* the ratio of the standard

deviations W_{n+1} and W_n is given from Equation 5 as $(n+1)/n$. Denoting by σ the standard deviation of eddy fluctuations at the reference level ($n=1$) the standard deviations of eddy fluctuations for successive stages of eddy growth are given as integer multiple of σ, *i.e.,* σ, 2σ, 3σ, etc. and correspond respectively to

statistical normalized standard deviation $t = 0,1,2,3,$ *etc.* (7)

The conventional power spectrum plotted as the variance versus the frequency in log-log scale will now represent the eddy probability density on logarithmic scale versus the standard deviation of the eddy fluctuations on linear scale since the logarithm of the eddy wavelength represents the standard deviation, *i.e.,* the r.m.s. value of eddy fluctuations (Equation 5). The r.m.s. value of eddy fluctuations can be represented in terms of statistical normal distribution as follows. A normalized standard deviation $t = 0$ corresponds to cumulative percentage probability density equal to 50 for the mean value of the distribution. Since the logarithm of the wavelength represents the r.m.s. value of eddy fluctuation the normalized standard deviation t is defined for the eddy energy as

$$T = (\log L/\log T_{50}) - 1 \quad (8)$$

where L is the period in units of time or space scale used in the analyses and T_{50} is the period up to which the cumulative percentage contribution to total variance is equal to 50 and $t = 0$. The variable $logT_{50}$ also represents the mean value for the r.m.s. eddy fluctuations and is consistent with the concept of the mean level represented by r.m.s. eddy fluctuations. Spectra of time series of any dynamical system, for example, meteorological parameters when plotted as cumulative percentage contribution to total variance versus t should follow the model predicted universal spectrum. The literature shows many examples of spectra of pressure, wind and temperature whose shapes display a remarkable degree of universality [Canavero and

Einaudi, 1987]. The theoretical basis for formulation of the universal spectrum is based on the *Central Limit Theorem in Statistics*, namely, if an overall random variable is the sum of very many elementary random variables, each having its own arbitrary distribution law, but all of them being small, then the distribution of the overall random variable is *Gaussian* [Ruhla, 1992]. Therefore, when the spectra of space-time fluctuations of dynamical systems are plotted in the above fashion, they tend to closely (not exactly) follow cumulative normal distribution.

The period T_{50} up to which the cumulative percentage contribution to total variance is equal to 50 is computed from model concepts as follows. The power spectrum, when plotted as normalized standard deviation t versus cumulative percentage contribution to total variance represents the statistical normal distribution (Equation 8), *i.e.,* the variance represents the probability density. The normalized standard deviation value *0* corresponds to cumulative percentage probability density P equal to 50 from statistical normal distribution characteristics. Since t represents the eddy growth step n (Equation 7), the dominant period T_{50} up to which the cumulative percentage contribution to total variance is equal to 50 is obtained from Equation 4 for value of n equal to 0. In the present study of periodicities in prime number spacing intervals, the primary perturbation time period T_s is equal to the unit number class interval (spacing interval between adjacent primes) and T_{50} is obtained as

$$T_{50} = (2 + \tau)\tau^{0} \sim 3.6 \text{ spacing interval between two adjacent primes} \quad (9)$$

Prime numbers with spacing intervals up to 3.6 or approximately 4 contribute up to 50% to the total variance. This model prediction is in agreement with computed value of T_{50} (Section 3.3).

2.2 Applications of model concepts to prime number distribution

The incorporation of *Fibonacci* mathematical series, representative of ramified bifurcations, indicates ordered growth of fractal patterns (Stewart, 1992). The fractal patterns are shown to result from the cumulative integration of enclosed small-scale fluctuations (Selvam and Suvarna Fadnavis, 1998). By analogy it follows that the *continuum number field* when computed as the integrated mean over successively larger discrete domains, also follows the quasiperiodic *Penrose* tiling pattern.

It is shown in the following that the steady state emergence of progressively larger fractal structures incorporate unique primary perturbation domains of progressively increasing total number equal to $z/\ln z$ where z, the length step growth stage is equal to the length scale ratio of large eddy to turbulent eddy.

In number theory, *prime numbers* are unique numbers and the *prime number theorem (PNT)* states that $z/\ln z$ gives approximately the number of *primes* less than or equal to z [Rose, 1995]. Historically, the *PNT* was postulated just before 1800 by both *Legendre* (1798) and *Gauss* (1791 in a personal communication) on numerical evidence and it was finally established by *Hadamard* and (independently) *de la Vallee Poussin* in 1896. The *PNT* states that if $\pi(z)$ is the number of primes p which satisfy $2 <= p <= z$ then $\pi(z)$ is approximately equal to $z/\ln z$ where ln represents the natural logarithm (Rose, 1995; Allenby and Redfern, 1989).

The *cell dynamical system model* for turbulent fluid flows predicts, as explained in the following, that the function $z/\ln z$ represents the normalized cumulative variance spectrum of the eddies and this spectrum follows *statistical normal distribution*.

The important result of the study is that the *prime number* spectrum is the same as the eddy energy spectrum for quantum-like chaos in atmospheric flows and the spectra follow the universal inverse power-law form of the statistical normal distribution.

The cell dynamical model concepts and its application to the evolution of prime number spectrum is explained in the following.

Large eddies are envelopes of enclosed turbulent eddy circulations, the relationship between root mean square (r.m.s.) circulation speeds W and w_* respectively of large and turbulent eddies of respective radii R and r is given as (Equation 3).

$$W^2 = \frac{2}{\pi}\frac{r}{R}w_*^2$$

In *number field* domain, the above equation can be visualized as follows. The r.m.s. circulation speeds W and w_* are equivalent to units of computations of respective *yardstick lengths* R and r. Spatial integration of w_* units of a finite yardstick length r, *i.e.,* a computational domain w_*r, results in a larger computational domain WR [Mary Selvam, 1993]. The computed domain WR is larger than the primary domain w_*r because of uncertainty in the length measurement using a finite yardstick length r, which should be infinitesimally small in an ideal measurement. The continuum number field domain (Cartesian co-ordinates) may therefore be obtained from successive integration of enclosed finite number field domains (Mary Selvam, 1993) as shown in Figure 1.

Cartesian co-ordinates represent the complex number field. Historically, Gauss (1799) clearly regarded a complex number as a pair of real numbers. The idea was originally stated in a little known work of a Danish surveyor Wessel (1797) and later by Gauss. In 1806, the French mathematician *Argand* described a complex number $x + iy$ as a point in the plane and this description was given the name 'Argand Diagram' [Stewart and Tall, 1990].

The above visualization (Figure 1) will help apply concepts developed for continuum atmospheric flow dynamics to evolution of

unique structures such as the distribution of prime numbers in real number field continuum, as explained in the following.

Fractal structures emerge in atmospheric flows because of mixing of environmental air into the large eddy volume by inherent turbulent eddy fluctuations. The steady state emergence of fractal structures A is equal to [Selvam and Suvarna Fadnavis, 1999a; b]

$$A = \frac{W R}{w_* r}$$

The spatial integration of enclosed turbulent eddy circulations as given in Equation (3) represents an overall logarithmic spiral flow trajectory with the quasiperiodic *Penrose* tiling pattern (Figure 2) for the internal structure [Selvam and Suvarna Fadnavis, 1999a; b] and is equivalent to a hierarchy of vortices (Section 2 above). The incorporation of *Fibonacci* mathematical series, representative of ramified bifurcations indicates ordered growth of fractal patterns and signifies non-local connections characteristic of quantum-like chaos. By analogy, the means of ensembles of successively larger *number field domains* follow a logarithmic spiral trajectory with the quasiperiodic *Penrose* tiling pattern (Figure 2) for the internal structure.

$$W = \frac{w_*}{k} \log z$$

where z is equal to the eddy length scale ratio R/r and k is equal to the steady state fractional volume dilution of large eddy by turbulent eddy fluctuations and is given as

$$k = \frac{w_* r}{W R} \tag{10}$$

The steady state emergence of fractal structure A is

$$A = \frac{W\,R}{w_*\,r} = \frac{W\,z}{w_*} \tag{11}$$

The outward and upward growing large eddy carries only a fraction f of the primary perturbation equal to

$$f = \frac{W}{w_*}\,\frac{r}{R}$$

because the fractional outward mass flux of primary perturbation equal to W/w_* occurs in the fractional turbulent eddy cross-section r/R.

$$f = \frac{\ln z}{k\,z} \qquad \text{from equation (5)}$$

$$= \frac{\ln z}{z}\left(\frac{W\,z}{w_*}\right) \qquad \text{from equation (10)}$$

$$= \frac{\ln z}{z}\sqrt{\frac{2}{\pi\,z}}\,z \qquad \text{from equation (3)}$$

Therefore

$$f = \sqrt{\frac{2}{\pi\,z}}\,\ln z \tag{12}$$

In atmospheric flows a fraction equal to f of surface air is transported upward to level z and represents the upward transport of moisture, which condenses as liquid water content in clouds, and also aerosols of surface origin. The observed vertical profile of liquid water content inside clouds is found to follow the f distribution [Mary Selvam and Ramachandra Murty, 1985; Mary Selvam, 1990]. The vertical profile of aerosol concentration in the atmosphere also

follows the *f* distribution [Sikka *et al.*, 1988]. The fraction *f* carries the unique signature of surface air (primary perturbation) at the level *z*.

The *f* distribution represents, at level *z*, the signature of unique primary perturbation originating from the underlying substratum. The *f* distribution therefore corresponds to the cumulative *prime number density distribution* corresponding to number *z*.

Therefore the ratio *P* equal to *A*/*f* gives the number of units of the unique domain of surface air at level *z*.

$$P = \frac{A}{f} = \frac{z}{\ln z} \tag{13}$$

In *number theory*, the Prime Number Theorem states that $z/\ln z$ where ln is the natural logarithm, represents approximately the number of primes less than or equal to *z*. *Prime numbers* are unique numbers, *i.e.,* which cannot be factorized [Stewart, 1996]. Therefore *P* represents the cumulative unique domain lengths of the primary perturbation carried up to the level *z*. In the next Section (3.0) the following model predictions (Section 2.0) are verified. (a) The *f* distribution represents the actual and computed prime number density distribution. (b) The power spectra (variance and phase) of prime number distribution follow the universal and unique inverse power-law form of the statistical normal distribution. Inverse power-law form for power spectra signify *self-similarity* or long-range correlations inherent to the eddy continuum. (c) The broadband eddy continuum exhibits dominant periodicities in close agreement with model predicted periodicities (Equation 4). (d) The variance and phase spectra follow each other closely, particularly for the dominant eddies, thereby exhibiting *'Berry's phase'* characterising quantum systems.

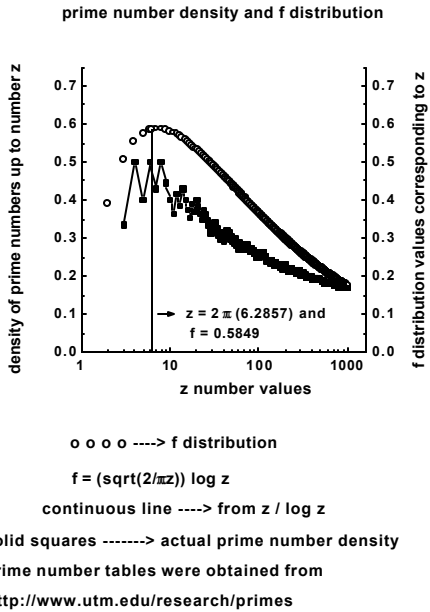

Figure 4: The cumulative prime number (actual) density and the corresponding *f* distribution have a maximum approximately equal to 0.6 for the number z equal to 2π which represents one complete eddy cycle. The eddy length scale ratio z represents the phase for the eddy continuum dynamics in turbulent fluid flows. A complete dominant eddy cycle ($z = 2\pi$) is a self-sustaining *soliton-like* structure.

3. Data and Analysis

The actual prime number tables (the first 1000 primes) were obtained from the web site: http://www.utm.edu/research/primes. The first 1000 prime numbers were used for the study. The prime numbers were also computed using the *Prime Number Theorem* proposed in 1799 by *Gauss*, namely the total number of primes $\pi(z)$ equal to or less than the number z is approximately equal to $z/\ln z$. The computed prime number density distribution is equal to $1/\ln z$.

The computed *f* distribution (Equation 12), the actual prime number density distribution and the computed prime number density distributions are shown in Figure 4.

The shape of the actual prime number density distribution is close to and resembles f distribution. Further, the maximum value (approximately equal to 0.6) for these two distributions occurs for z value equal to 2π. The eddy length scale ratio z represents the phase (Section 2) and therefore the maximum values for f and also (by analogy), for the prime number distributions occur for one complete cycle of eddy circulation. Such a closed self-sustaining circulation is similar to a *soliton*, a stable self-sustaining eddy structure.

3.1 The Frequency Distributions of Prime numbers, f Distribution *and* the Statistical Normal Distribution

The values of actual prime number distribution, the corresponding values computed using the relation $z/\ln z$ (Prime Number Theorem) which give the *number of primes* less *than or equal to* z and the f distribution follow *statistical normal distribution* (Selvam and Suvarna Fadnavis, 2001) as described in the following. The frequency distributions were computed in terms of the normalised standard deviation as explained in the following for prime number (calculated) distribution. The number of *primes* p less than z are calculated for a range of n values from $x_1 = z_1$ to $x_n = z_n$. The cumulative percentage number of primes p_c is calculated as equal to $(p_m/p_n)*100$ where $m = 1,2,...n$ for each class interval $X = (x_m + x_{m+1})/2$. The number of primes $p_t = p_{m+1} - p_m$ in each class interval X is also calculated. The normalized standard deviate t is then equal to $(Xbar - X)/\sigma$ where $Xbar$ is the mean of the prime number distribution. The corresponding standard deviation of the X versus p_t distribution is then calculated as equal to σ.

The prime number (actual and computed) frequency distribution and also the corresponding f distribution for values of z from 3 to 1000 at unit intervals are shown in Figure 5. The statistical normal distribution is also plotted in the Figure 5. It is seen that the prime

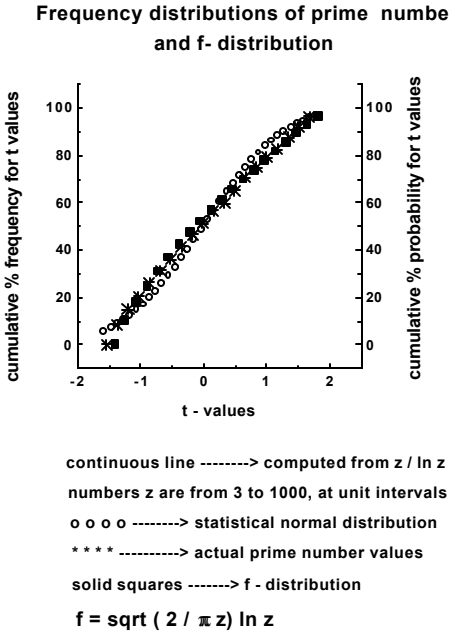

Figure 5: Prime number (actual and computed) distribution and corresponding *f* distribution follow closely the statistical normal distribution.

number (actual and computed) distributions and the corresponding *f* distribution closely follow statistical normal distribution.

3.2 Spectra of prime number distribution

In the quantum-like chaos in atmospheric flows the function $z/\ln z$ represents the variance spectrum of the fractal structures as shown below.

The length scale ratio z equal to R/r represents the relative variance (Equation 3). The relative upward mass flux of primary perturbation equal to W/w_* is proportional to $\ln z$ (Equation 5). Therefore $z/\ln z$ represents the cumulative variance normalized to upward flow of primary perturbation. The cumulative variance or energy spectrum of the eddies is therefore represented by $z/\ln z$ distribution.

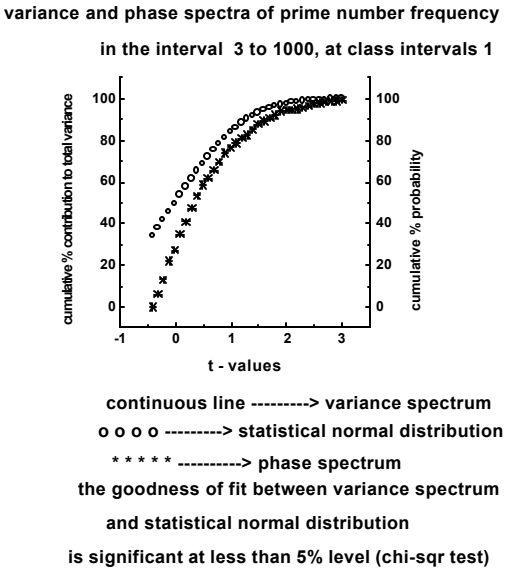

Figure 6: The variance and phase spectra along with statistical normal distribution.

By concept (Equation 3) large eddies are but the integrated mean of inherent turbulent eddies and therefore the eddy energy spectrum follows statistical normal distribution according to the *Central Limit Theorem* (Section 2.1(e) above). The *prime number* spectrum, which is equivalent to the variance (energy) spectrum of eddies follows statistical *normal distribution* as seen in Figure 5. Earlier studies using various meteorological data sets have shown that atmospheric eddy energy spectrum follow statistical normal distribution [Selvam and Suvarna Fadnavis, 1998].

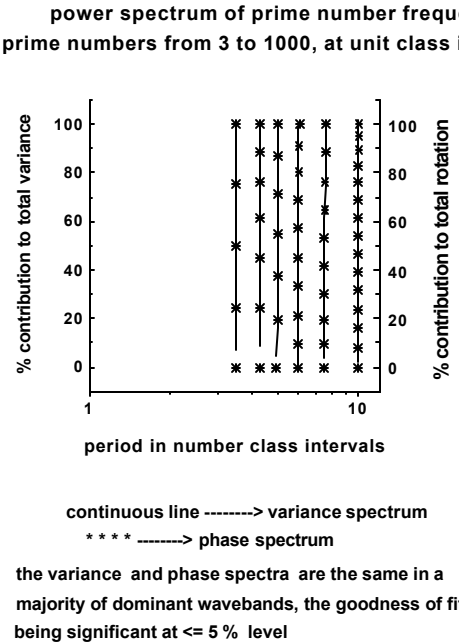

Figure 7a: Illustration of *Berry*'s phase in quantum-like chaos in prime number distribution. The phase and variance spectra are the same for prime number spacing intervals up to 10.

3.3 Power Spectral Analysis: Analyses Techniques, Data and Results

The broadband power spectrum of space-time fluctuations of dynamical systems can be computed accurately by an elementary, but very powerful method of analysis developed by *Jenkinson* (1977) which provides a quasi-continuous form of the classical periodogram allowing systematic allocation of the total variance and degrees of freedom of the data series to logarithmically spaced elements of the frequency range (0.5, 0). The periodogram is constructed for a fixed set of 10000(m) periodicities L_m which increase geometrically as $L_m = 2 \exp(Cm)$ where $C = .001$ and $m = 0, 1, 2, \ldots m$. The data series

Y_t for the N data points was used. The periodogram estimates the set of $A_m cos(2\pi\nu_m S - \phi_m)$ where A_m, ν_m and ϕ_m denote respectively the amplitude, frequency and phase angle for the m^{th} periodicity and S is the time or space interval. In the present study the frequency of occurrence of primes in *unit number class intervals* ranging from 3 to 1000 was used. The cumulative percentage contribution to total variance was computed starting from the high frequency side of the spectrum. The period T_{50} at which 50% contribution to total variance occurs is taken as reference and the normalized standard deviation t_m values are computed as (Equation 8).

$$t_m = (\log L_m / \log T_{50}) - 1$$

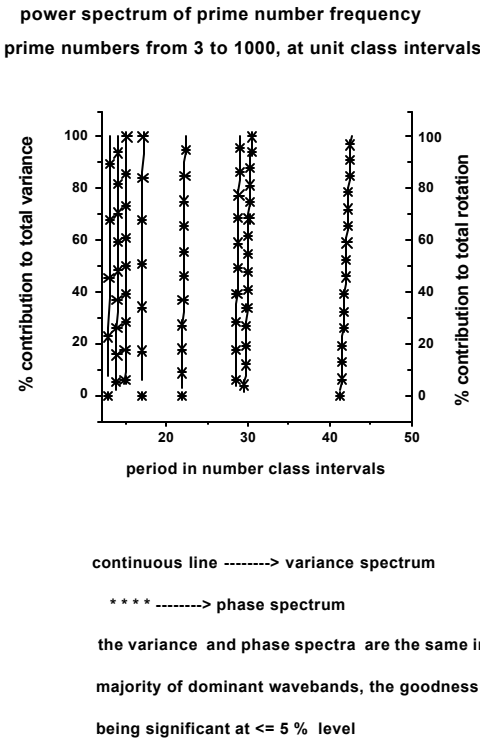

Figure 7b: Illustration of *Berry*'s phase in quantum-like chaos in prime number distribution. The phase and variance spectra are the same for prime number spacing intervals from 10 to 50.

The cumulative percentage contribution to total variance, the cumulative percentage normalized phase (normalized with respect to the total phase rotation) and the corresponding t values were computed. The power spectra were plotted as cumulative percentage contribution to total variance versus the normalized standard deviation t as given above. The period L is in units of number class interval which is equal to *one* in the present study. Periodicities up to T_{50} contribute up to 50% of total variance. The phase spectra were plotted as cumulative (%) normalized (normalized to total rotation)

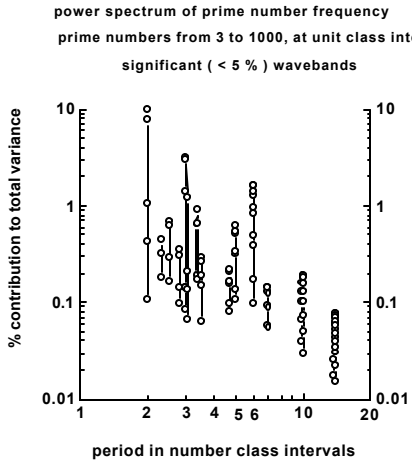

Figure 8: Continuous periodogram analysis results: Dominant (normalised variance greater than 1) statistically significant wavebands.

The significant(< 5 %) wavebands (in unit class intervals) are :

(1) 2.0 - 2.006 (2) 2.01 (3) 2.331 - 2.335

(4) 2.497 - 2.505 (5) 2.796 - 2.804 (6) 2.987 - 3.014

(7) 3.327 - 3.341 (8) 3.491 - 3.505 (9) 4.656 - 4.679

(10) 4.984 - 5.014 (11) 5.972 - 6.026 (12) 6.974 - 7.023

(13) 9.926 - 10.066 (14) 13.876 - 14.128

phase. The variance and phase spectra along with statistical normal distribution is shown in Figure 6. The 'goodness of fit' between the variance spectrum and statistical normal distribution is significant at <= 5% level. The phase spectrum is close to the statistical normal distribution, but the 'goodness of fit' is not statistically significant. However, the 'goodness of fit' between variance and phase spectra are statistically significant (chi-square test) for individual dominant wavebands (Figures 7a and 7b).

The cumulative percentage contribution to total variance and the cumulative (%) normalized phase (normalized w.r.t. the total rotation) for each dominant waveband is computed for significant wavebands

and shown in Figures 7a and 7b to illustrate *Berry's phase*, namely the progressive increase in phase with increase in period and also the close association between phase and variance (see Section 2).

The statistically significant (less than or equal to 5% level) wavebands are shown in Figure 8.

Table 1 (see Appendix) gives the list of a total of 110 dominant (normalised variance greater than 1) wavebands obtained from the continuous periodogram analyses for the data set (prime numbers in the interval 3 to 1000 at unit class intervals). The symbol * indicates that the dominant waveband is statistically significant at <= 5% level. There are 14 significant dominant wavebands (Figure 8). The dominant peak periodicities are in close agreement with model predicted dominant peak periodicities, *e.g.*, 2.2, 3.6, 5.8, 9.5, 15.3, 24.8, 40.1, and 64.9 prime number spacing intervals for values of n ranging from –1 to 6 (Equation 4). The symbol **S** indicates that the normalised variance and phase spectra follow each other closely (the '*goodness of fit* ' being significant at <= 5%) displaying *Berry* 's phase in the quantum-like chaos exhibited by prime number distribution. Earlier study by Marek Wolf (May 1996, IFTUWr 908/96 http://rose.ift.uni.wroc.pl/~mwolf) also shows that the number of *Twins* (spacing interval 2) and primes separated by a gap of length 4 ("*cousins*") is almost the same and it determines a fractal structure on the set of primes. The conjecture that there should be approximately equal numbers of prime power pairs differing by 2 and by 4, but about twice as many differing by 6 is proved to be true by Gopalkrishna Gadiyar and Padma (1999 http://www.maths.ex.ac.uk /~mwatkins/zeta/padma.pdf). The dominant perodicities shown above at Figure 8 are consistent with these reported results. The period T_{50} up to which the cumulative percentage contribution to total variance is equal to 50 is found to be equal to 3.242 spacing interval between two adjacent primes. This periodogram estimate of T_{50} for the prime

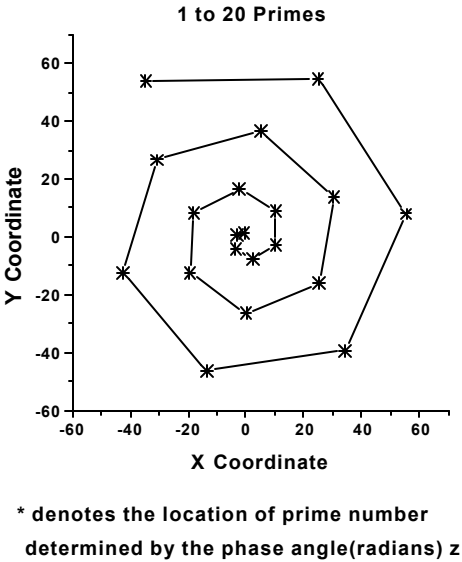

Figure 9: The spiral pattern traced in the *x-y* plane by the first *20* prime numbers.

numbers in the interval 3 to 1000 is in approximate agreement with model predicted value of T_{50} approximately equal to 3.6 (Equation 9). The dominant significant period 2 corresponds to *twin primes*. In *number theory* [Rose, 1995; Beiler, 1966] the *twin prime conjecture* states that there are many pairs of primes p, q where $q = p + 2$. There are infinitely many prime pairs as z tends to infinity.

3.4 Spiral Pattern of Prime Number Distribution in the *x-y* Plane

The z^{th} prime is approximately equal to $z \ln z$ [Allenby and Redfern, 1989]. In the following it is shown that the prime numbers are arranged in a spiral pattern in the *x-y* plane. The equiangular logarithmic spiral shown at Figure 3 is given by the relation

$$R/r = e^{\alpha\theta}$$

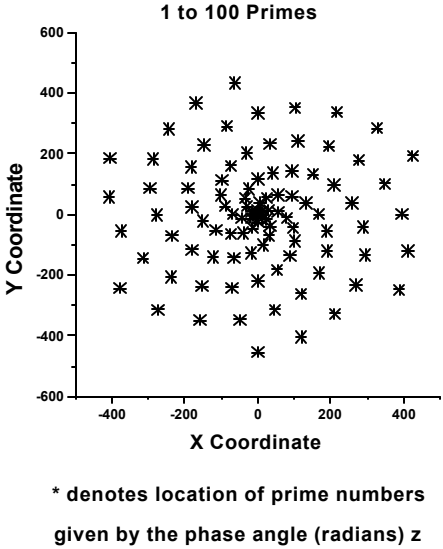

Figure 10: The location in the *x-y* plane of the first *100* prime numbers. The spiralling arms closely resemble *phyllotaxis-like* patterns such as that seen in the familiar spiral patterns found in the arrangement of leaves on a stem, in florets of composite flowers, the pattern of scales on pineapple and pine cone, *etc*., http://xxx.lanl.gov/abs/chao-dyn/9806001.

Since the eddy length scale ratio z is equal to R/r

$$\ln z = \alpha\theta = (1/z)(1/z)$$

$$z\ln z = 1/z = r/R = d\theta$$

The z^{th} prime number has an angular phase difference equal to $1/z$ radians from the earlier $(z-1)^{th}$ prime. The spiral arrangement of the first 20 and 100 primes are shown respectively in Figures 9 and 10. Spiral patterns in the arrangement of prime numbers have been reported earlier by mathematicians (Schroeder, 1986; also shown in the website http://zaphod.uchicago.edu/~bryan/spiral/index.html).

4. Conclusions

In mathematics, Cantorian fractal space-time fluctuations is now associated with reference to quantum systems [Ord, 1983; Nottale,

1989; El Naschie, 1993; 1998]. Recent studies indicate a close association between *number theory* in mathematics, in particular, the distribution of *prime numbers* and the chaotic orbits of excited quantum systems such as the hydrogen atom [Cipra, 1996; Berry, 1992; Cipra http://www.maths.ex.ac.uk/~mwatkins/zeta/cipra.htm]. The spacing intervals of adjacent prime numbers exhibit *fractal* fluctuations generic to diverse dynamical systems in nature. The irregular (chaotic) *fractal* fluctuations however, exhibit *self-similar* geometry manifested as inverse power-law form for power spectra. *Self-similar* fluctuations imply long-range correlations or non-local connections identified as *self-organized criticality*. A cell dynamical system model for atmospheric flows developed by the author shows that *self-organized criticality* is a signature of quantum-like chaos. The cell dynamical system model is a general systems theory applicable to all dynamical systems in nature. The model concepts show that quantum-like chaos in dynamical systems incorporates *prime number distribution functions* in the quantification of *self-organized criticality*. The model also provides unique quantification for the observed *self-organized criticality* in terms of the universal statistical normal distribution.

The important result of the present study is that power spectra of different data sets of spacing intervals of adjacent prime numbers follow the model predicted universal inverse power-law form of the statistical normal distribution, a signature of *self-organized criticality*. The prime number distribution therefore exhibits quantum-like chaos.

Acknowledgements

The author is grateful to Dr. A. S. R. Murty for his keen interest and encouragement during the course of the study.

References

Allenby, R. B. J. T. and Redfern, E. J., 1989: *Introduction to Number Theory with Computing*. Routledge, Chapman and Hall Inc., NY, pp.310.

Bak, P. C., Tang, C. and Wiesenfeld, K., 1988: Self-organized criticality. *Phys. Rev. A* **38**, 364-374.

Beiler, A. H., 1966: *Recreations in the Theory of Numbers-The Queen of Mathematics*. Dover Publications Inc., pp. 339.

Berry, M. V., 1988: The geometric phase. *Sci. Amer*. **Dec**., 26-32.

Berry, M., 1992: Quantum Physics on the edge of Chaos. In *The New Scientist Guide to Chaos* (Ed.) Nina Hall, Penguin Books, U.K., pp. 184 -195.

Canavero, F. G., Einaudi, F., 1987: Time and space variability of atmospheric processes. *J. Atmos. Sci*. **44(12)**, 1589-1604.

Cipra, B., 1996: Prime formula weds number theory and quantum physics. *Science* **274**, 2014-1015.

Cipra, B., http://www.maths.ex.ac.uk/~mwatkins/zeta/cipra.htm A prime case of chaos. *What's happening in the Mathematical Sciences*, **Vol. 4**.

Devlin, K., 1997: *Mathematics: The Science of Patterns.* Scientific American Library, NY, p.101.

El Naschie, M. S., 1993: Penrose tiling, semi-conduction and Cantorian $1/f^{\alpha}$ spectra in four and five dimensions. *Chaos, Solitons and Fractals* **3(4)**, 489-491.

El Naschie, M. S., 1998: Penrose universe and Cantorian *space-time* as a model for noncommutative quantum geometry. *Chaos, Solitons and Fractals* **9(6)**, 931-934.

Ghil, M., 1994: Cryothermodynamics: The chaotic dynamics of paleoclimate, *Physica D* **77**,130-159.

Gleick, J., 1987: *Chaos: Making a New Science*, Viking, New York.

Gopalakrishna Gadiyar, H. and Padma, R., 1999: Ramanujan-Fourier Series, the Wiener-Khintchine formula and the distribution of prime pairs. *Physica A* **269**, 503-510. http://www.maths.ex.ac.uk/~mwatkins/zeta/padma.pdf

Jean R.V. 1994. *Phyllotaxis : A systemic Study in Plant Morphogenesis*, Cambridge University Press, NY, USA.

Keating, J., 1990: Physics and the queen of mathematics. *Physics World* **April**, 46-50.

Klarreich, E., 2000: Prime time. *New Scientist* **11 November**, 32-36.

Klir, G. J., 1992: Systems science: a guided tour. *J. Biological Systems* **1**, 27-58.

Lorenz, E. N., 1963: Deterministic non-periodic flow. *J. Atmos. Sci*. **20**, 130-141.

Maddox, J., 1988: Licence to slang Copenhagen? *Nature* **332**, 581.

Mary Selvam, A., and Ramachandra Murty, A. S., 1985: Numerical simulation of warm rain process. *Proc. of the 4th WMO Scientific Conf. on Weather Modification* 12-14 August 1985, Honolulu, Hawaii, 503-506.

http://xxx.lanl.gov/abs/physics/9911021

Mary Selvam, A., 1990: Deterministic chaos, fractals and quantumlike mechanics in atmospheric flows. *Can. J. Phys.* **68**, 831-841.

http://xxx.lanl.gov/html/physics/0010046

Mary Selvam, A., 1993: Universal quantification for deterministic chaos in dynamical systems. *Applied Math. Modelling* **17**, 642-649.

http://xxx.lanl.gov/html/physics/0008010

Mathews, G. B., 1961: *Theory of Numbers*. Chelsea Publishing Company, New York, pp.321.

Nottale, L., 1989: Fractals and the quantum theory of space-time. *Int'l. J. Mod. Phys. A* **4(19)**, 5047-5117.

Ord, G. N., 1983: Fractal space-time: a geometric analogue of relativistic quantum mechanics. *J. Phys.A: Math. Gen.* **16**, 1869-1884.

Peacocke, A. R., 1989: *The Physical Chemistry of Biological Organization*, Clarendon Press, Oxford, U.K.

Poincaré, H., 1892: *Les Methodes Nouvelle de la Mecannique Celeste*. Gauthier-Villars, Paris.

Rose, H. E., 1995: *A Course in Number Theory*. Second Edition, Oxford Science Publications, Clarendon Press, Oxford, pp.395.

Ruhla, C. 1992: *The Physics of Chance*. Oxford University Press, Oxford, pp.217.

Schroeder, M. R. 1986: *Number Theory in Science and Communication*. Second enlarged edition, Springer-Verlag, New York, pp.367.

Seife, C., 1998: Into the vortex. *New Scientist* **24 Oct**., p.7.

Selvam A. M. and Suvarna Fadnavis, 1998: Signatures of a universal spectrum for atmospheric interannual variability in some disparate climatic regimes. *Meteorology and Atmospheric Physics* **66**, 87-112. (http://xxx.lanl.gov/abs/chao-dyn/9805028)

Selvam A. M. and Suvarna Fadnavis, 1999a: Superstrings, Cantorian-fractal Space-time and quantum-like chaos in atmosperic flows. *Chaos, Solitons and Fractals* **10(8)**, 1321 - 1334. (http://xxx.lanl.gov/abs/chao-dyn/9806002).

Selvam A. M. and Suvarna Fadnavis, 1999b: Cantorian fractal *space-time*, quantum-like chaos and scale relativity in atmospheric flows. *Chaos, Solitons and Fractals* **10(9)**, 1577 - 1582. (http://xxx.lanl.gov/abs/chao-dyn/9808015).

Selvam A. M. and Suvarna Fadnavis, 2001: Cantorian Fractal Patterns, Quantum-like Chaos and Prime Numbers in Atmospheric Flows. http://xxx.lanl.gov/abs/chao-dyn/9810011 (to be submitted for Journal publication).

Sikka, P., Mary selvam, A., and Ramachandra Murty, A. S., 1988: Possible solar influence on atmospheric electric field. *Adv. Atmos. Sci.* **2**, 218-118. (http://xxx.lanl.gov/abs/chao-dyn/9806014).

Stewart, I. and Tall, D. 1990: *The Foundations of Mathematics*. Oxford University Press, Oxford, pp.261.

Stewart, I., 1992: Where do nature's patterns come from ?, *Nature* **135**, 14.

Stewart, I., 1996: *From here to infinity*. Oxford University Press, Oxford, pp. 299.

Stewart, I. 1998: *Life's other secret*. The Penguin Press, England, pp.270.

Townsend, A. A., 1956: *The Structure of Turbulent Shear Flow*. Cambridge University Press, Cambridge, London, U.K., pp.115 -130.

Wallace, J. M., Hobbs, P. V. 1977: *Atmospheric Science: An Introductory Survey*. Academic Press, N.Y.

Wolf, M. May 1996: Unexpected regularities in the distribution of prime numbers. IFTUWr 908/96. http://rose.ift.uni.wroc.pl/~mwolf

Appendix

Table 1: The list of a total of 110 dominant (normalised variance greater than 1) wavebands obtained from the continuous periodogram analyses for the data set (prime numbers in the interval 3 to 1000 at unit class intervals)

No	Periodicities in unit number class intervals	
	Peak period	Wave band
1	2.000	2.000 to 2.006 *
2	2.010	2.010..to..2.010 *
3	2.014	2.014..to..2.014
4	2.022	2.022..to..2.022
5	2.034	2.034..to..2.034
6	2.077	2.077..to..2.077
7	2.100	2.098..to..2.100
8	2.113	2.113..to..2.113
9	2.136	2.136..to..2.136
10	2.143	2.141..to..2.145
11	2.149	2.149..to..2.149
12	2.164	2.164..to..2.164
13	2.199	2.197..to..2.199
14	2.235	2.235..to..2.235
15	2.266	2.264..to..2.266
16	2.307	2.305..to..2.310
17	2.333	2.331..to..2.335 *
18	2.356	2.356..to..2.356
19	2.364	2.364..to..2.366
20	2.445	2.443..to..2.448

21	2.467	2.467..to..2.470
22	2.500	2.497..to..2.505 *
23	2.615	2.615..to..2.617
24	2.625	2.623..to..2.628
25	2.657	2.654..to..2.657
26	2.711	2.708..to..2.711
27	2.727	2.724..to..2.730
28	2.749	2.746..to..2.752
29	2.801	2.796..to..2.804 *
30	2.890	2.890..to..2.890
31	2.925	2.925..to..2.925
32	2.936	2.933..to..2.936
33	2.969	2.969..to..2.969
34	2.999	2.987..to..3.014 *
35	3.023	3.023..to..3.023
36	3.050	3.047..to..3.050
37	3.143	3.143..to..3.146
38	3.252	3.252..to..3.252
39	3.288	3.288..to..3.288
40	3.297	3.294..to..3.301
41	3.334	3.327..to..3.341 *
42	3.347	3.347..to..3.351
43	3.361	3.361..to..3.364
44	3.456	3.442..to..3.456
45	3.470	3.470..to..3.473
46	3.498	3.491.to..3.505 *S
47	3.537	3.537.to..3.540
48	3.558	3.558..to..3.558
49	3.666	3.663..to..3.670
50	3.688	3.685..to..3.688
51	3.714	3.707..to..3.722

52	3.748	3.744..to..3.755
53	3.782	3.778..to..3.782
54	3.820	3.816..to..3.823
55	3.881	3.881..to..3.881
56	4.125	4.125..to..4.125
57	4.200	4.196..to..4.204
58	4.247	4.242..to..4.247
59	4.285	4.281..to..4.294
60	4.333	4.320..to..4.346 S
61	4.372	4.367..to..4.376
62	4.402	4.394..to..4.407
63	4.568	4.568..to..4.568
64	4.600	4.596..to..4.605
65	4.670	4.656..to..4.679 *
66	4.717	4.717..to..4.722
67	4.750	4.745..to..4.760
68	4.774	4.769..to..4.779
69	4.939	4.934..to..4.944
70	4.964	4.964..to..4.969
71	4.999	4.984..to..5.014 * S
72	5.034	5.034..to..5.034
73	5.084	5.074..to..5.094
74	5.161	5.161..to..5.161
75	5.197	5.192..to..5.197
76	5.250	5.250..to..5.250
77	5.497	5.491..to..5.502
78	5.813	5.802..to..5.819
79	5.913	5.907..to..5.919
80	5.949	5.943..to..5.960
81	6.002	5.972..to..6.026 *S
82	6.051	6.044..to..6.057

83	6.087	6.081..to..6.087
84	6.124	6.124..to..6.130
85	6.279	6.272..to..6.285
86	6.329	6.323..to..6.329
87	6.496	6.489..to..6.502
88	6.995	6.974..to..7.023 *
89	7.346	7.324..to..7.361
90	7.509	7.472..to..7.539 S
91	7.638	7.615..to..7.653
92	8.102	8.086..to..8.119
93	8.399	8.366..to..8.425
94	8.501	8.484..to..8.526
95	9.986	9.926..to..10.066 * S
96	10.540	10.508..to..10.571
97	10.981	10.915..to..11.036
98	12.977	12.912..to..13.029 S
99	13.212	13.212..to..13.226
100	14.001	13.876..to..14.128 * S
101	15.031	14.897..to..15.152 S
102	15.458	15.412..to..15.505
103	17.050	16.948..to..17.153 S
104	22.113	21.871..to..22.335 S
105	28.793	28.450..to..29.025 S
106	29.998	29.581..to..30.452 S
107	31.223	31.192..to..31.254
108	42.020	41.353..to..42.655 S
109	198.57	192.702..to..204.414 S
110	1534.7	965.984..to..3402.097 S